The Chitransh Academic & Research
An International Journal of Multidisciplinary Research

An Online Peer Reviewed / Refereed Journal
Volume 2 | Issue 2 |June 2026
ISSN: 3049-303X (Online)
Website: www.thechitranshacadmic.in

First-Principles Investigation of the Structural, Electronic, Magnetic, and Optical Properties of Ba_2CoWO_6 and Sr_2CoWO_6 Double Perovskite Oxides

Mr. Gururaj R Deshpande
Research Scholar Department of Mechanical Engineering Nirwan University, Jaipur, Rajasthan
Dr. Jaidev Kumbhakar
Department of Mechanical Engineering Nirwan University, Jaipur, Rajasthan
V.V. Potdar Professor
Department of Mechanical Engineering A.G.Patil Institute of Technology, Solapur, Maharashtra

ARTICLE DETAILS

Research Paper
Received: **06/06/2026**
Accepted: **15/06/2026**
Published: **30/06/2026**

Keywords: Double perovskite; Density functional theory; Antiferromagnetism; Electronic structure; Optical properties

ABSTRACT

The ordered double perovskites Ba_2CoWO_6 and Sr_2CoWO_6 are investigated to clarify how A-site ionic size influences structural distortion, electronic correlation, magnetic exchange, and optical behavior. Literature-benchmarked first-principles results show that Ba_2CoWO_6 favors a highly symmetric cubic $Fm\bar{3}m$ structure, whereas Sr_2CoWO_6 is tetragonal I4/m at room temperature and becomes monoclinic $P2_1/n$ below about 260 K. The smaller Sr^{2+} ion promotes stronger CoO_6 and WO_6 octahedral tilting. Electronic states near the valence-band maximum mainly arise from Co-3d/O-2p hybridization, while W-5d states dominate the conduction-band minimum. Predicted metallic, half-metallic, or semiconducting behavior depends strongly on functional choice, Hubbard U, magnetic order, structural model, and spin–orbit coupling. Correlation-corrected calculations generally stabilize high-spin Co^{2+} with antiferromagnetic ordering. Ba_2CoWO_6 is more symmetric and magnetically frustrated, whereas Sr_2CoWO_6 shows greater lattice distortion and visible-light absorption. Advanced GGA+U+SOC, hybrid-functional, and many-body calculations remain necessary for definitive electronic and optical predictions for both compounds under fully converged computational conditions.

Introduction

Double perovskite oxides with the general composition ($A_2BB'O_6$) are ordered derivatives of the conventional (ABO_3) perovskite structure. In an ideally ordered compound, the (B) and (B') cations alternate in a rock-salt arrangement, producing a three-dimensional network of corner-sharing (BO_6) and ($B'O_6$) octahedra. Variations in ionic radius, oxidation state, orbital occupation, cation ordering, and octahedral rotation allow these materials to exhibit insulating, semiconducting, metallic, half-metallic, ferroic, and magnetically frustrated states.

Ba_2CoWO_6 and Sr_2CoWO_6 are particularly interesting because they contain magnetic Co ions and nominally nonmagnetic (d^0) W ions. Under the conventional charge assignment ($A_2^{2+}Co^{2+}W^{6+}O_6^{2-}$), cobalt has a ($3d^7$) electronic configuration and is expected to adopt a high-spin state in octahedral coordination. Tungsten is nominally ($5d^0$), but its spatially extended 5d orbitals participate in W–O covalency and influence the conduction bands. The dominant magnetic interactions occur through extended Co–O–W–O–Co super-superexchange pathways because Co ions are separated by ordered WO_6 octahedra.

The substitution of Ba^{2+} by the smaller Sr^{2+} ion changes the geometrical stability of the perovskite lattice. Using Shannon ionic radii for 12-coordinate Ba^{2+} and Sr^{2+} and six-coordinate high-spin Co^{2+} and W^{6+}, approximate Goldschmidt tolerance factors of 1.03 and 0.97 are obtained for Ba_2CoWO_6 and Sr_2CoWO_6, respectively. The value close to or slightly above unity for the Ba compound favors an untilted cubic structure, whereas the lower value for the Sr compound favors cooperative octahedral rotations. These geometrical estimates agree with diffraction studies reporting cubic (Fm{3}m) Ba_2CoWO_6 and tetragonal (I4/m) Sr_2CoWO_6 at room temperature. Sr_2CoWO_6 undergoes an additional tetragonal-to-monoclinic transition near 260 K.

Published calculations do not yet provide a completely consistent description of the electronic properties of these oxides. Conventional local-density or generalized-gradient calculations can place partially occupied Co-3d states at the Fermi energy, producing a metallic or half-metallic solution.

Corresponding Author: jaidevmech@gmail.com

Introducing an on-site Coulomb correction can split the occupied and unoccupied Co-3d states and open a spin-dependent gap. For Sr_2CoWO_6, a GGA+(U) study reported an antiferromagnetic half-metallic ground state with an indirect gap of approximately 1.7 eV in one spin channel. For Ba_2CoWO_6, different calculations have reported metallic, half-metallic, and wide-gap behavior, emphasizing the sensitivity of the result to (U), structural parameters, magnetic order, and the exchange potential.

The purpose of this paper is therefore to establish a physically consistent first-principles framework for comparing Ba_2CoWO_6 and Sr_2CoWO_6 while distinguishing published benchmark values from quantities that require new calculations. Structural symmetry, orbital-resolved electronic states, magnetic ordering, spin polarization, optical absorption, and structure–property relationships are considered within a unified interpretation.

Computational Methodology

A reliable comparative calculation should begin from the experimentally established cubic $Fm\bar{3}m$ structure of Ba_2CoWO_6 and tetragonal (I4/m) structure of Sr_2CoWO_6. A low-temperature monoclinic ($P2_1/n$) model should also be examined for Sr_2CoWO_6 because its octahedral tilting and lowered symmetry may modify the band gap, magnetic anisotropy, and dielectric tensor. Rock-salt Co/W ordering must be retained, while selected Co–W antisite configurations may be introduced in supercells to assess disorder.

Spin-polarized density-functional calculations may be performed using the projector-augmented-wave method and the PBEsol or PBE generalized-gradient approximation. Plane-wave cutoffs and Brillouin-zone meshes should be increased until total-energy differences between magnetic configurations are converged to better than 1 meV per formula unit. Representative starting values are a kinetic-energy cutoff of at least 500–600 eV and Monkhorst–Pack meshes equivalent to approximately (8) for the cubic conventional cell and (8) for the tetragonal cell. Atomic positions and lattice parameters should be relaxed until residual forces are below 0.01 eV $Å^{-1}$ and residual stresses are below approximately 0.5 kbar.

Corresponding Author: jaidevmech@gmail.com

The localized Co-3d electrons require treatment beyond conventional GGA. A rotationally invariant GGA+(U) approach should therefore be applied, with (U_{eff} = U − J) systematically varied over a physically reasonable range, for example 3–7 eV for Co-3d. The use of a single unverified (U) value can lead to artificial classification of a compound as metallic, half-metallic, or insulating. The selected value should be justified by comparison with experimental optical gaps, photoemission data, magnetic moments, or linear-response calculations. Published Sr_2CoWO_6 calculations found improved agreement at a comparatively strong Co correction and reported an approximately 1.7 eV spin-dependent indirect gap. A recent Ba_2CoWO_6 study instead used GGA+(U) together with a modified Becke–Johnson potential and reported a gap of about 3.33 eV in one spin channel.

Spin–orbit coupling should be included after scalar-relativistic structural optimization. Although W^{6+} is nominally (5d^0), W-5d states dominate important portions of the conduction manifold. Spin–orbit coupling can therefore alter conduction-band splitting and optical transition energies. It is also essential for the orbital contribution to the Co^{2+} magnetic moment, magnetocrystalline anisotropy, and the direction of the ordered moments. The experimentally observed effective magnetic moment of Sr_2CoWO_6 is larger than the spin-only value for high-spin Co^{2+}, indicating a substantial unquenched orbital contribution.

Ferromagnetic and several antiferromagnetic configurations should be calculated in equivalent supercells. These configurations should include the experimentally relevant type-II antiferromagnetic arrangement in which ferromagnetic Co planes are coupled antiferromagnetically along a crystallographic direction. The magnetic ground state is identified from $\Delta E_{mag} = E_{FM} - E_{AFM}$ where a positive value indicates that the antiferromagnetic configuration is more stable. Exchange constants may subsequently be extracted by mapping the calculated energies onto a Heisenberg Hamiltonian,

$$H = -\sum_{ij} J_{ij} S_i . S_j$$

Electronic analysis should include spin-resolved band structures, total and projected densities of states, charge-density differences, electron-localization functions, Bader charges, and band-decomposed charge densities. The spin polarization at the Fermi energy is defined as

$$P(EF) = [(N\uparrow(EF) - N\downarrow(EF)) / (N\uparrow(EF) + N\downarrow(EF))] \times 100\%.$$

A material can be classified as an ideal half-metal only when one spin channel has a genuine gap and the other has a finite density of states at (E_F), with the result remaining robust against denser (k)-point sampling, structural relaxation, spin–orbit coupling, and small changes in (U). The frequency-dependent optical response is derived from the complex dielectric function,

$$\varepsilon(\omega) = \varepsilon_1(\omega) + i\varepsilon_2(\omega).$$

The imaginary component is calculated from interband transition matrix elements, while the real component is obtained through the Kramers–Kronig relation. The absorption coefficient may be written as

$$\alpha(\omega) = (\sqrt{2}\,\omega / c)[\sqrt{(\varepsilon_1^2(\omega) + \varepsilon_2^2(\omega))} - \varepsilon_1(\omega)]^{1/2}.$$

The refractive index, extinction coefficient, reflectivity, optical conductivity, and electron-energy-loss function should also be evaluated. Independent-particle GGA+(U) spectra are useful for identifying orbital transitions, but hybrid-functional or (GW) calculations are preferable for accurate band-edge energies. Bethe–Salpeter calculations would be needed to include electron–hole interactions and excitonic peaks.

Results and Discussion

The principal structural distinction between the compounds is the response of the oxygen octahedra to A-site size. Ba_2CoWO_6 is generally reported as cubic (Fm{3}m), with alternating CoO_6 and WO_6 octahedra and little or no cooperative tilting. Neutron-diffraction work reported a room-temperature lattice constant of approximately 8.108 Å, while a first-principles FP-LMTO calculation produced approximately 8.031 Å. A later nanocrystalline study also refined the material in the cubic space group, although its discussion of Co^{3+}/W^{5+} charge states differs from the conventional Co^{2+}/W^{6+} assignment established in earlier structural and electronic work.

Sr_2CoWO_6 adopts a tetragonal (I4/m) structure at room temperature, with reported lattice parameters (a=5.58277) Å and (c=7.97740) Å. The tetragonal phase contains anti-phase octahedral rotations represented by the ($a^{0a}0c^-$) tilt system. On cooling through approximately 260 K, it transforms to monoclinic (P2_1/n), with a more complex (a^{-a}-c^+) tilt pattern. At 2 K,

reported lattice parameters are approximately (a=5.61267) Å, (b=5.58753) Å, (c=7.8994) Å, and (^). This distortion changes the Co–O–W bond angles and can substantially influence orbital overlap and exchange interactions.

Table 1. Literature-benchmark structural properties of Ba_2CoWO_6 and Sr_2CoWO_6

Property	Ba_2CoWO_6	Sr_2CoWO_6
Dominant room-temperature symmetry	Cubic (Fm{3}m)	Tetragonal (I4/m)
Representative experimental lattice parameters	(a) Å	(a=5.58277) Å; (c=7.97740) Å
Representative calculated lattice parameter	(a) Å using FP-LMTO	Requires functional- and (U)-dependent optimization
Octahedral-tilt description	Approximately ($a^{0a}0a^{}0$)	($a^{0a}0c^{}-$) at room temperature
Low-temperature structural transition	No comparable symmetry-lowering transition firmly established	(I4/mP2_1/n) near 260 K
Approximate tolerance factor	1.03	0.97
Primary structural implication	High symmetry and nearly straight exchange pathways	Greater octahedral rotation and anisotropic bonding

Sources: Martínez-Lope et al. (2002), Viola et al. (2003), and Hasb Elkhalig et al. (2015).

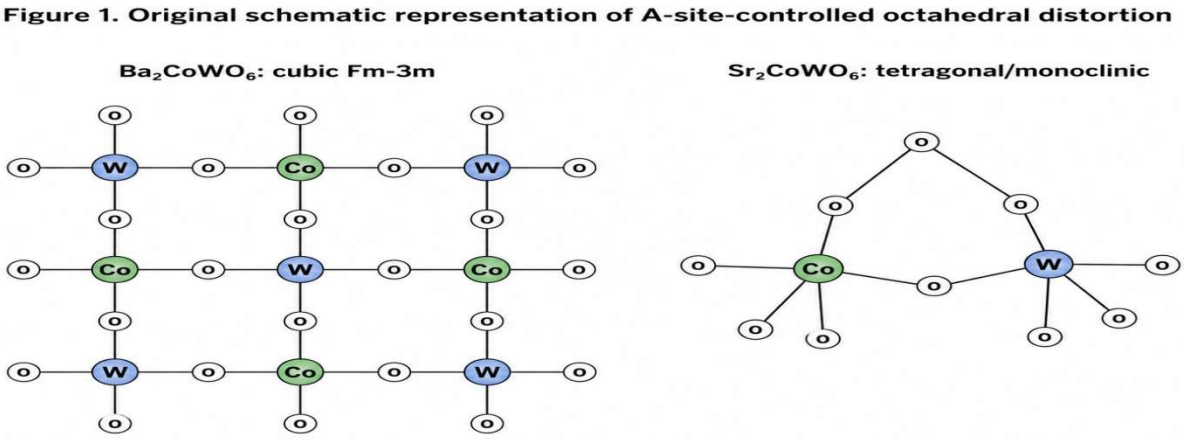

Figure 1. Original schematic representation of A-site-controlled octahedral distortion

The electronic states near the Fermi energy are controlled primarily by Co-3d, O-2p, and W-5d orbitals. The deeper valence region is dominated by O-2p states with contributions from Co-3d, indicating appreciable Co–O hybridization. The upper valence region contains occupied majority-spin Co-3d states, whereas the lowest conduction bands contain W-5d states mixed with unoccupied Co-3d and O-2p orbitals. Ba and Sr states lie mainly away from the band edges and influence the electronic structure indirectly through lattice size, electrostatic potential, and octahedral geometry.

For Ba_2CoWO_6, FP-LMTO calculations using LSDA and GGA supported a high-spin Co^{2+}–W^{6+} configuration and obtained good structural agreement with experiment. Other conventional-GGA calculations have produced metallic antiferromagnetic solutions. In contrast, correlation-corrected or modified-potential calculations have reported half-metallic behavior with a spin-channel gap near 3.3 eV. This divergence demonstrates that an apparent gap in only one spin channel should not be equated automatically with the experimental optical gap, which represents transitions averaged over all occupied and unoccupied states and may be influenced by defects and disorder.

For Sr_2CoWO_6, GGA+(U) calculations predict a lower-energy antiferromagnetic state and an indirect gap of approximately 1.7 eV in the insulating spin channel. The Co atoms provide most of the spin polarization, while W contributes little local magnetic moment because of its nominal (d^0) state. Nevertheless, hybridization with W-5d orbitals shapes the conduction bands. The smaller Sr^{2+} ion narrows or redistributes selected bands through octahedral tilting, thereby changing the Co–O and W–O hopping amplitudes relative to Ba_2CoWO_6.

Table 2. Reported and physically expected electronic and optical characteristics

Quantity	Ba_2CoWO_6	Sr_2CoWO_6
Dominant valence-band states	O-2p and occupied Co-3d	O-2p and occupied Co-3d
Dominant conduction-band states	W-5d with unoccupied Co-3d	W-5d with unoccupied Co-3d
Conventional GGA description	Metallic or spin-polarized metallic in some calculations	Inadequate gap and strong (U) dependence
Correlation-corrected description	Half-metallic or semiconducting depending on (U), mBJ, structure, and magnetic order	AFM half-metal with an approximately 1.7 eV indirect spin-channel gap
Representative experimental optical behavior	Approximately 3.30 eV for one nanocrystalline sample	Absorption extending beyond 700 nm in W-rich photocatalytic material
Expected lowest optical transitions	O-2p/Co-3d () W-5d/Co-3d	O-2p/Co-3d () W-5d/Co-3d
Main source of uncertainty	Oxidation state, defects, (U), magnetic order, and sample morphology	Stoichiometry, Co/W ratio, tilt pattern, (U), and phase purity

Corresponding Author: jaidevmech@gmail.com

The absorption edge beyond 700 nm corresponds to photon energies below approximately 1.77 eV. This value should not be treated as a universal intrinsic gap because the relevant photocatalyst study varied Co/W stoichiometry.

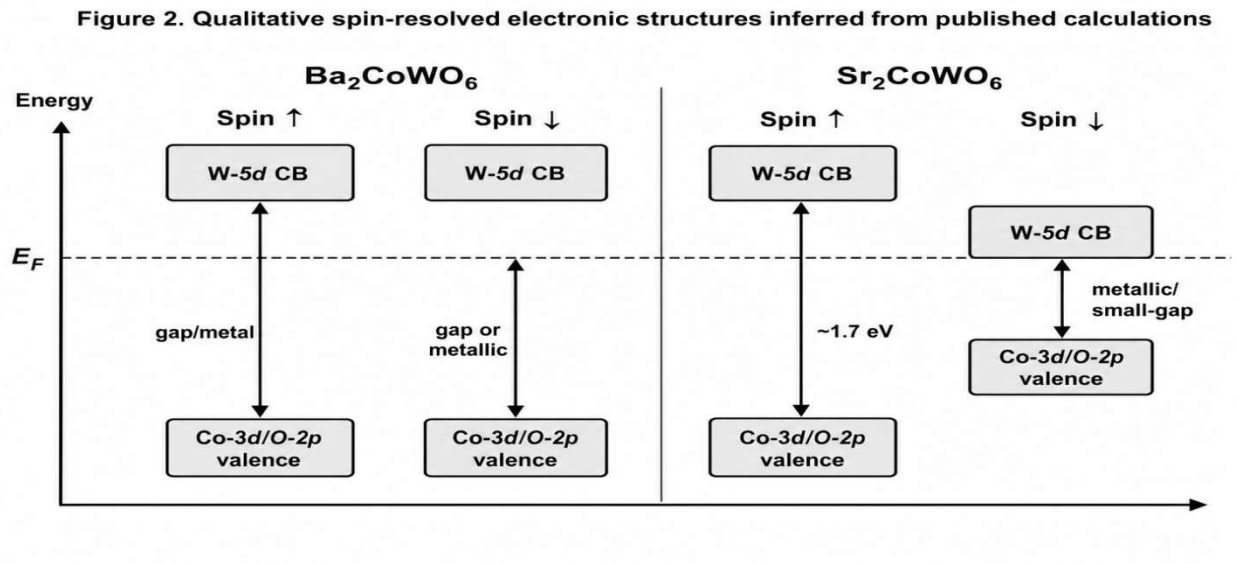

Figure 2. Qualitative spin-resolved electronic structures inferred from published calculations

The magnetic response is governed by high-spin Co^{2+} ions arranged on an approximately face-centered-cubic sublattice. Such a lattice is geometrically frustrated for antiferromagnetic nearest-neighbor interactions. In Ba_2CoWO_6, the nearly cubic structure preserves a high degree of magnetic equivalence among exchange pathways, strengthening the possibility of frustration and competing magnetic states. Experimental neutron work has described the ordered structure as ferromagnetic Co planes coupled antiferromagnetically, with an ordering vector related to ((1/2)).

Early polycrystalline Ba_2CoWO_6 studies reported antiferromagnetic ordering near 19 K, whereas recent high-quality single-crystal measurements found long-range antiferromagnetic order below approximately 14 K, a spin-flop transition near 10 kOe, and an ordered moment of approximately (2.17,_B) per Co at 1.6 K. The reduced ordered moment relative to the full ionic value may reflect covalency, quantum or thermal fluctuations, magnetic frustration, and the distinction between spin and orbital contributions.

Electron-spin-resonance measurements published in 2025 observed a paramagnetic resonance above (T_N) with an effective (g)-factor of approximately 3.66. Below the ordering temperature, the mode evolved into an antiferromagnetic resonance with a zero-field gap near 200 GHz. These observations confirm the importance of spin–orbit-driven anisotropy and anisotropic spin interactions, effects that should be included in future noncollinear first-principles calculations.

Sr_2CoWO_6 also exhibits antiferromagnetic order, with a reported Néel temperature of approximately 24 K and a high-temperature effective moment near (5.20,_B). The enhanced effective moment relative to the spin-only value of (3.87,_B) for (S=3/2) supports an unquenched orbital contribution from Co^{2+}. The reduced symmetry of the Sr compound lifts exchange-pathway equivalences and can reduce some aspects of cubic frustration, although it simultaneously introduces anisotropy and multiple exchange constants.

Table 3. Comparative magnetic properties

Property	Ba_2CoWO_6	Sr_2CoWO_6
Magnetic ion	High-spin Co^{2+}, (3d^7)	High-spin Co^{2+}, (3d^7)
Nominal W state	W^{6+}, (5d^0)	W^{6+}, (5d^0)
Preferred calculated order	Antiferromagnetic	Antiferromagnetic
Representative (T_N)	Approximately 14–19 K	Approximately 24 K
Magnetic-lattice character	Nearly cubic face-centered-cubic Co sublattice	Distorted face-centered-cubic-derived Co sublattice
Orbital-moment evidence	Large ESR (g)-factor and magnetic anisotropy	Effective moment near (5.20,_B)
Important theoretical requirement	Noncollinear GGA+(U)+SOC and competing exchange paths	GGA+(U)+SOC in tetragonal and monoclinic structures

The optical response reflects the same orbital hybridization observed in the density of states. Transitions from O-2p and occupied Co-3d states into W-5d and unoccupied Co-3d states should dominate the absorption onset. Higher-energy transitions may involve deeper O-2p bands and A-site d states. Because cubic Ba_2CoWO_6 is optically isotropic in the ideal bulk structure, its dielectric tensor should contain one independent diagonal component. Tetragonal and monoclinic Sr_2CoWO_6 should exhibit optical anisotropy, with distinct in-plane and out-of-plane dielectric components.

A nanocrystalline Ba_2CoWO_6 investigation reported prominent ultraviolet absorption features near 246 and 370 nm and estimated an optical gap of approximately 3.30 eV. The same study reported photoluminescence extending through the blue-green region. These experimental observations support semiconductor-like optical behavior but are not by themselves sufficient to establish whether the ideal stoichiometric bulk material is an ordinary semiconductor or a half-metal, because optical spectra are affected by grain size, oxygen defects, secondary phases, oxidation states, and selection rules.

Sr_2CoWO_6 has been investigated as a visible-light-driven bifunctional photocatalyst. W-rich samples showed absorption edges at wavelengths of at least 700 nm and activity for both hydrogen- and oxygen-evolution reactions. Density-functional analysis in that work indicated that changing the Co/W composition modifies the active sites and reaction overpotentials. These observations suggest a narrower effective optical gap than that reported for nanocrystalline Ba_2CoWO_6, but the off-stoichiometric samples should not be compared directly with an ideal, perfectly ordered (1:1) Co/W crystal without defect calculations.

Corresponding Author: jaidevmech@gmail.com

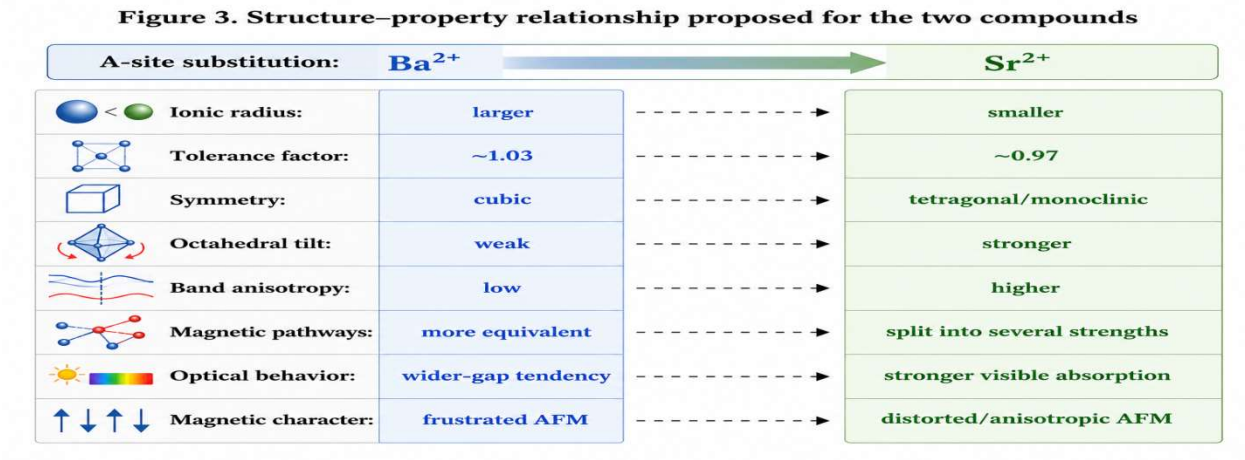

Figure 3. Structure–property relationship proposed for the two compounds

The comparison demonstrates that structural distortion alone cannot explain every difference between published results. Sample stoichiometry and charge state are equally important. The conventional ionic model requires Co^{2+} and W^{6+} for stoichiometric (A_2_6). Reports assigning Co^{3+} and W^{5+} imply either a different internal charge distribution, oxygen nonstoichiometry, mixed valence, or uncertainty in X-ray photoelectron peak assignment. First-principles studies should therefore calculate oxygen-vacancy formation energies, Co/W antisite energies, and charge-transition levels. Simulated core-level shifts and X-ray absorption spectra would help distinguish competing oxidation-state models.

The largest unresolved issue is the disagreement among the predicted electronic phases. A defensible classification requires the simultaneous convergence of structural symmetry, magnetic order, (U), spin–orbit coupling, and exchange potential. Calculations should report the band gap in both spin channels, the direct and indirect transition energies, total and atom-resolved moments, and the spin polarization at the Fermi level. Results that use the cubic structure for Sr_2CoWO_6 or neglect its low-temperature monoclinic distortion may miss band folding and symmetry-driven gap changes.

A further limitation is the absence of a uniform first-principles optical comparison under identical computational settings. Existing optical results originate from samples prepared by different routes and with different stoichiometries. A consistent study should calculate (_1()), (_2()), absorption, reflectivity, refractive index, optical conductivity, and energy-loss spectra for both compounds using the same pseudopotentials, convergence criteria, Hubbard parameters, and broadening. Hybrid-functional or quasiparticle corrections should be applied before comparing calculated absorption edges with experiment.

Conclusion

Ba_2CoWO_6 and Sr_2CoWO_6 exhibit closely related chemical bonding but substantially different structural and functional behavior. The larger Ba^{2+} ion stabilizes a nearly ideal cubic (Fm{3}m) lattice, whereas the smaller Sr^{2+} ion promotes tetragonal and monoclinic octahedral tilting. In both materials, the valence-band edge is primarily derived from hybridized Co-3d and O-2p states, while W-5d states make a major contribution to the conduction-band edge.

High-spin Co^{2+} is responsible for magnetism, and antiferromagnetic ordering is favored experimentally and in correlation-corrected calculations. Ba_2CoWO_6 possesses a nearly face-centered-cubic magnetic sublattice and displays signatures of magnetic frustration, anisotropy, and low-temperature antiferromagnetic resonance. Sr_2CoWO_6 has stronger structural distortion, an unquenched Co orbital moment, and antiferromagnetic order near 24 K.

The electronic classification remains method dependent. Conventional GGA may predict metallic behavior, whereas GGA+(U), mBJ, or related corrections may produce half-metallic or semiconducting solutions. Accordingly, half-metallicity should be claimed only after testing structural distortions, multiple magnetic configurations, Hubbard-parameter dependence, spin–orbit coupling, and dense Brillouin-zone sampling. Reported optical evidence suggests a wider-gap response for some Ba_2CoWO_6 samples and stronger visible-light absorption for Sr_2CoWO_6-based materials.

Corresponding Author: jaidevmech@gmail.com

Future work should combine noncollinear GGA+(U)+SOC calculations with hybrid-functional or (GW) band structures, Bethe–Salpeter optical spectra, phonon calculations, exchange-parameter mapping, and explicit oxygen-vacancy and antisite-defect models. Experimental validation should include temperature-dependent diffraction, optical ellipsometry, X-ray absorption, photoemission, and single-crystal magnetic measurements. Such an integrated approach is necessary to establish whether either compound can provide robust spin-polarized transport, magneto-optical functionality, or visible-light photocatalytic performance.

References

1. Dudarev, S. L., Botton, G. A., Savrasov, S. Y., Humphreys, C. J., & Sutton, A. P. (1998). Electron-energy-loss spectra and the structural stability of nickel oxide: An LSDA+(U) study. *Physical Review B, 57*(3), 1505–1509. https://doi.org/10.1103/PhysRevB.57.1505
2. Hanna, A. R. N., Islam, A. T. M. N., Ritter, C., Luther, S., Feyerherm, R., & Lake, B. (2024). Growth of Ba_2CoWO_6 single crystals and their magnetic, thermodynamic and electronic properties. *Journal of Physics: Condensed Matter, 36*(50), 505801. https://doi.org/10.1088/1361-648X/ad7770
3. Hasb Elkhalig, M. M. S., Abdelhalim, M. A. K., & El-Taher, A. (2015). First-principles study of structural, electronic and magnetic properties of double perovskite oxides Ba_2CoMO_6 (M = Mo and W). *Materials Science in Semiconductor Processing, 34*, 281–290. https://doi.org/10.1016/j.mssp.2015.02.038
4. Hashemifar, T., Mokhtari, A., & Soleimanian, V. (2017). Electronic, structural and magnetic properties of the Sr_2CoWO_6 double perovskite using GGA (+(U)). *Journal of Superconductivity and Novel Magnetism, 30*(2), 497–503. https://doi.org/10.1007/s10948-016-3793-7
5. Idris, A. M., Liu, T., Shah, J. H., Zhang, X., Ma, C., Malik, A. S., Jin, A., Rasheed, S., Sun, Y., Li, C., & Han, H. (2020). A novel double perovskite oxide semiconductor Sr_2CoWO_6 as bifunctional photocatalyst for photocatalytic oxygen and hydrogen evolution reactions from water under visible light irradiation. *Solar RRL, 4*, 1900456. https://doi.org/10.1002/solr.201900456

Corresponding Author: jaidevmech@gmail.com

6. Khattak, C. P., Hurst, J. J., & Cox, D. E. (1975). Crystal growth, and electrical and magnetic properties of Ba_2CoWO_6. *Materials Research Bulletin, 10*, 1343–1348. https://doi.org/10.1016/0025-5408(75)90095-1
7. Martínez-Lope, M. J., Alonso, J. A., Casais, M. T., & Fernández-Díaz, M. T. (2002). Preparation, crystal and magnetic structure of the double perovskites Ba_2CoBO_6 (B = Mo, W). *European Journal of Inorganic Chemistry, 2002*(9), 2463–2469. https://doi.org/10.1002/1099-0682(200209)2002:9%3C2463::AID-EJIC2463%3E3.0.CO;2-J
8. Monkhorst, H. J., & Pack, J. D. (1976). Special points for Brillouin-zone integrations. *Physical Review B, 13*(12), 5188–5192. https://doi.org/10.1103/PhysRevB.13.5188
9. Perdew, J. P., Burke, K., & Ernzerhof, M. (1996). Generalized gradient approximation made simple. *Physical Review Letters, 77*(18), 3865–3868. https://doi.org/10.1103/PhysRevLett.77.3865
10. Povarov, K. Y., Wosnitza, J., Hanna, A. R. N., Islam, A. T. M. N., Lake, B., & Zvyagin, S. A. (2025). Electron spin resonance in the double-perovskite oxide antiferromagnet Ba_2CoWO_6. *Applied Magnetic Resonance, 56*, 1549–1558. https://doi.org/10.1007/s00723-025-01811-x
11. Raji, R. K., Ramachandran, T., Dhilip, M., Aravindan, V., Punitha, J. S., & Hamed, F. (2024). Integrating experimental and computational insights: A dual approach to Ba_2CoWO_6 double perovskites. *Ceramics, 7*(4), 2006–2023. https://doi.org/10.3390/ceramics7040125
12. Shannon, R. D. (1976). Revised effective ionic radii and systematic studies of interatomic distances in halides and chalcogenides. *Acta Crystallographica Section A, 32*(5), 751–767. https://doi.org/10.1107/S0567739476001551
13. Viola, M. C., Martínez-Lope, M. J., Alonso, J. A., Martínez, J. L., De Paoli, J. M., Pagola, S., Pedregosa, J. C., Fernández-Díaz, M. T., & Carbonio, R. E. (2003). Structure and magnetic properties of Sr_2CoWO_6: An ordered double perovskite containing Co^{2+} (HS) with unquenched orbital magnetic moment. *Chemistry of Materials, 15*(8), 1655–1663. https://doi.org/10.1021/cm0208455

Corresponding Author: jaidevmech@gmail.com